Article:

Díaz-Martínez, Paloma, Maestre, Fernando T., Moreno-Jiménez, Eduardo et al. (124 more authors) (2024) Vulnerability of mineral-associated soil organic carbon to climate across global drylands. Nature Climate Change. pp. 976-982. ISSN 1758-678X

https://doi.org/10.1038/s41558-024-02087-y

Vulnerability of mineral-associated soil organic carbon to climate across global drylands

Paloma Díaz-Martínez[1], Fernando T. Maestre[2], Eduardo Moreno-Jiménez[3,4], Manuel Delgado-Baquerizo[5], David J. Eldridge[6], Hugo Saiz[7], Nicolas Gross[8], Yoann Le Bagousse-Pinguet[9], Beatriz Gozalo[10], Victoria Ochoa[10], Emilio Guirado[10], Miguel García-Gómez[11], Enrique Valencia[12], Sergio Asensio[10], Miguel Berdugo[12], Jaime Martínez-Valderrama[10,13], Betty J. Mendoza[14], Juan C. García-Gil[1], Claudio Zaccone[15], Marco Panettieri[1], Pablo García-Palacios[1,16], Wei Fan[17], Iria Benavente-Ferraces[1], Ana Rey[18], Nico Eisenhauer[19,20], Simone Cesarz[19,20], Mehdi Abedi[21], Rodrigo J. Ahumada[22], Julio M. Alcántara[23], Fateh Amghar[24], Valeria Aramayo[25], Antonio I. Arroyo[26], Khadijeh Bahalkeh[21], Farah Ben Salem[27], Niels Blaum[28], Bazartseren Boldgiv[29], Matthew A. Bowker[30,31], Donaldo Bran[25], Cristina Branquinho[32], Chongfeng Bu[33], Yonatan Cáceres[34], Rafaella Canessa[35], Andrea P. Castillo-Monroy[36], Ignacio Castro[37], Patricio Castro-Quezada[38], Roukaya Chibani[39], Abel A. Conceição[40], Courtney M. Currier[41,42], Anthony Darrouzet-Nardi[43], Balázs Deák[44], Christopher R. Dickman[45], David A. Donoso[36], Andrew J. Dougill[46], Jorge Durán[47], Hamid Ejtehadi[48], Carlos Espinosa[49], Alex Fajardo[50], Mohammad Farzam[51,52], Daniela Ferrante[53], Lauchlan H. Fraser[54], Juan J. Gaitán[55,56], Elizabeth Gusman Montalván[49], Rosa M. Hernández-Hernández[37], Andreas von Hessberg[57], Norbert Hölzel[58], Elisabeth Huber-Sannwald[59], Frederic M. Hughes[60,40,61], Oswaldo Jadán-Maza[38], Katja Geissler[28], Anke Jentsch[57], Mengchen Ju[33,62], Kudzai F. Kaseke[63], Liana Kindermann[64], Jessica E. Koopman[65], Peter C. Le Roux[66], Pierre Liancourt[67,68], Anja Linstädter[64,69], Jushan Liu[70], Michelle A. Louw[66], Gillian Maggs-Kölling[71], Thulani P. Makhalanyane[72], Oumarou Malam Issa[73], Eugene Marais[71], Pierre Margerie[74], Antonio J. Mazaneda[75], Mitchel P. McClaran[76], João Vitor S. Messeder[77], Juan P. Mora[50], Gerardo Moreno[34], Seth M. Munson[78], Alice Nunes[32], Gabriel Oliva[53,69], Gastón R. Oñatibia[79], Brooke Osborne[80], Guadalupe Peter[55,81], Yolanda Pueyo[26], R. Emiliano Quiroga[22,82], Sasha C. Reed[83], Victor M. Reyes[84], Alexandra Rodríguez[47], Jan C. Ruppert[68], Osvaldo Sala[41,85,42], Ayman Salah[86], Julius Sebei[87], Michael Sloan[30], Shijirbaatar Solongo[88], Ilan Stavi[89], Colton R.A. Stephens[54], Alberto L. Teixido[12], Andrew D. Thomas[90], Heather L. Throop[91,41], Katja Tielbörger[68], Samantha Travers[6], James Val[92], Orsolya Valko[44], Liesbeth van den Brink[68,93], Frederike Velbert[58], Wanyoike Wamiti[94], Deli Wang[70], Lixin Wang[95], Glenda M. Wardle[45], Laura Yahdjian[79], Eli Zaady[96,97], Juan M. Zeberio[81], Yuanming Zhang[98], Xiaobing Zhou[98], César Plaza[1]

[1]Instituto de Ciencias Agrarias (ICA), CSIC, Madrid, Spain.[2]Environmental Sciences and Engineering, Biological and Environmental Science and Engineering Division, King Abdullah University of Science and Technology, Thuwal, Kingdom of Saudi Arabia.[3]Department of Agricultural and Food Chemistry, Faculty of Sciences, Universidad Autónoma de Madrid, Madrid, Spain.[4]Institute for Advanced Research in Chemical Sciences, Madrid, Spain.[5]Laboratorio de Biodiversidad y Funcionamiento Ecosistémico, Instituto de Recursos Naturales y Agrobiología de Sevilla (IRNAS), CSIC, Sevilla, Spain.[6]Centre for Ecosystem Science, School of Biological, Earth and Environmental Sciences, University of New South Wales, Sydney, New South Wales, Australia.[7]Institut de Biología Evolutiva, UPF-CSIC,

Barcelona, Spain.[8]Université Clermont Auvergne, INRAE, VetAgro Sup, Unité Mixte de Recherche Ecosystème Prairial, Clermont-Ferrand, France.[9]Aix Marseille Univ, CNRS, Avignon Université, IRD, IMBE, Aix-en-Provence, France.[10]Instituto Multidisciplinar para el Estudio del Medio "Ramón Margalef", Universidad de Alicante, Alicante, Spain.[11]Departamento de Ingeniería y Morfología del Terreno, Escuela Técnica Superior de Ingenieros de Caminos, Canales y Puertos, Universidad Politécnica de Madrid, Madrid, Spain.[12]Departamento de Biodiversidad, Ecología y Evolución, Facultad de Ciencias Biológicas, Universidad Complutense de Madrid, Madrid, Spain.[13]Estación Experimental de Zonas Áridas (EEZA), CSIC, Almería, Spain.[14]Departamento de Biología y Geología, Física y Química Inorgánica, Universidad Rey Juan Carlos, Madrid, Spain.[15]Department of Biotechnology, University of Verona, Verona, Italy.[16]Department of Plant and Microbial Biology, University of Zurich, Zurich, Switzerland.[17]Institute of Agricultural Environment and Resources, Jilin Academy of Agricultural Sciences, Changchun, China.[18]Museo Nacional de Ciencias Naturales (MNCN), CSIC, Madrid, Spain.[19]German Centre for Integrative Biodiversity Research (iDiv) Halle-Jena-Leipzig, Leipzig, Germany.[20]Leipzig University, Institute of Biology, Leipzig, Germany.[21]Department of Range Management, Faculty of Natural Resources and Marine Sciences, Tarbiat Modares University, Noor, Mazandaran Province, Iran.[22]Instituto Nacional de Tecnología Agropecuaria, Estación Experimental Agropecuaria Catamarca, Catamarca, Argentina.[23]Instituto Interuniversitario de Investigación del Sistema Tierra en Andalucía, Universidad de Jaén, Jaén, Spain.[24]Laboratoire de Recherche: Biodiversité, Biotechnologie, Environnement et Développement Durable (BioDev), Faculté des Sciences, Université M'hamed Bougara de Boumerdès, Boumerdès, Algérie.[25]Instituto Nacional de Tecnología Agropecuaria (INTA), Estación Experimental Agropecuaria Bariloche. Bariloche, Río Negro, Argentina.[26]Instituto Pirenaico de Ecología (IPE), CSIC, Zaragoza, Spain.[27]Laboratory of Pastoral Ecosystems and Promotion of Spontaneous plants and Associated Microorganisms, Institut des Régions Arides (IRA) Médenine, Tunisia.[28]University of Potsdam, Plant Ecology and Nature Conservation, Potsdam, Germany.[29]Laboratory of Ecological and Evolutionary Synthesis, Department of Biology, School of Arts and Sciences, National University of Mongolia, Ulaanbaatar, Mongolia.[30]School of Forestry, Northern Arizona University, Flagstaff, AZ, USA.[31]Center for Ecosystem Science and Society, Northern Arizona University, Flagstaff, AZ, USA.[32]Center for Ecology, Evolution and Environmental Changes (cE3c) & CHANGE - Global Change and Sustainability Institute, Faculdade de Ciências, Universidade de Lisboa, Campo Grande, Lisboa, Portugal.[33]Institute of Soil and Water Conservation, Northwest Agriculture and Forestry University, Yangling, Shaanxi, China.[34]Forestry School, INDEHESA, Universidad de Extremadura, Plasencia, Spain.[35]Ecological Plant Geography, Faculty of Geography, University of Marburg, Marburg, Germany.[36]Grupo de Investigación en Ecología y Evolución en los Trópicos-EETrop-Universidad de las Américas, Campus Udlapark, Quito, Ecuador.[37]Universidad Nacional Experimental Simón Rodríguez (UNESR), Instituto de Estudios Científicos y Tecnológicos (IDECYT), Centro de Estudios de Agroecología Tropical (CEDAT), Laboratorio de Biogeoquímica, Miranda, Venezuela.[38]Universidad de Cuenca, Facultad de Ciencias Agropecuarias, Carrera de Ingeniería Agronómica, Grupo de Agroforestería, Manejo y Conservación del paisaje, Ecuador.[39]Laboratory of Eremology and Combating Desertification; Institut des Régions Arides (IRA), Médenine, Tunisia.[40]Universidade Estadual de Feira de Santana, Departamento de Ciências Biológicas, Feira de Santana, Bahia, Brazil.[41]School of Life Sciences, Arizona State University, Tempe, AZ, USA.[42]Global Drylands Center, Arizona State University, Tempe, AZ, USA.[43]Department of Biological Sciences, University of Texas at El

Paso, El Paso, TX, USA.[44]Lendület Seed Ecology Research Group, Institute of Ecology and Botany, HUN-REN Centre for Ecological Research, Vácrátót, Hungary.[45]Desert Ecology Research Group, School of Life and Environmental Sciences, The University of Sydney, Sydney, New South Wales, Australia.[46]School of Earth and Environment, University of Leeds, Leeds, UK.[47]Misión Biológica de Galicia (MBG), CSIC, Pontevedra, Spain.[48]Quantitative Plant Ecology and Biodiversity Research Lab., Department of Biology, Faculty of Science, Ferdowsi University of Mashhad, Mashhad, Iran.[49]Departamento de Ciencias Biológicas, Universidad Técnica Particular de Loja, Loja, Ecuador.[50]Instituto de Investigación Interdisciplinaria (I3), Universidad de Talca, Talca, Chile.[51]Department of Range and Watershed Management, Ferdowsi University of Mashhad, Mashhad, Iran.[52]Department of Molecular and Life Sciences, Curtin University, Australia.[53]Universidad Nacional de la Patagonia Austral, Río Gallegos, Santa Cruz, Argentina.[54]Department of Natural Resource Science, Thompson Rivers University, British Columbia, Canada.[55]Consejo Nacional de Investigaciones Científicas y Técnicas de Argentina (CONICET), Buenos Aires, Argentina.[56]Departamento de Tecnología, Universidad Nacional de Luján, Buenos Aires, Argentina.[57]Department of Disturbance Ecology, Bayreuth Center of Ecology and Environmental Research BayCEER, University of Bayreuth, Bayreuth, Germany.[58]Institute of Landscape Ecology, University of Münster, Münster, Germany.[59]Instituto Potosino de Investigación Científica y Tecnológica, A.C., SLP, Mexico.[60]Universidade Estadual de Santa Cruz, Conselho de Curadores das Coleções Científicas and Zoologia, Ilhéus, Bahia, Brazil.[61]Universidade Federal de Minas Gerais, Bioinformática, Belo Horizonte, Minas Gerais, Brazil.[62]Yangling Vocational & Technical College, Yangling, Shaanxi, China.[63]Earth Research Institute, University of California Santa Barbara, CA, USA.[64]University of Potsdam, Institute of Biochemistry and Biology, Biodiversity Research / Systematic Botany, Potsdam, Germany.[65]Centre for Microbial Ecology and Genomics, Department of Biochemistry, Genetics and Microbiology, University of Pretoria, Pretoria, South Africa.[66]Department of Plant and Soil Sciences, University of Pretoria, Pretoria, South Africa.[67]Institute Botany Department, State Museum of Natural History Stuttgart, Stuttgart, Germany.[68]Plant Ecology Group, University of Tübingen, Tübingen, Germany.[69]Institute of Crop Science and Resource Conservation, University of Bonn, Bonn, Germany.[70]Key Laboratory of Vegetation Ecology of the Ministry of Education, Jilin Songnen Grassland Ecosystem National Observation and Research Station, Institute of Grassland Science, Northeast Normal University, Changchun, China.[71]Gobabeb-Namib Research Institute, Walvis Bay, Namibia.[72]Department of Microbiology and the School of Data Science and Computational Thinking, Faculty of Science, Stellenbosch University, Stellenbosch, South Africa.[73]Institut d'Écologie et des Sciences de l'Environnement de Paris (iEES-Paris), Sorbonne Université, IRD, CNRS, INRAE, Université Paris Est Creteil, Université de Paris, France.[74]Normandie Univ, UNIROUEN, INRAE, ECODIV, Rouen, France.[75]Departamento de Biología Animal, Biología Vegetal y Ecología, Universidad de Jaén, Jaén, Spain.[76]School of Natural Resources and the Environment, University of Arizona, Tucson, AZ, USA.[77]Biology Department & Ecology Program, The Pennsylvania State University, University Park, PA, USA.[78]US Geological Survey, Southwest Biological Science Center, Flagstaff, AZ, USA.[79]Cátedra de Ecología, Facultad de Agronomía, Universidad de Buenos Aires, Instituto de Investigaciones Fisiológicas y Ecológicas Vinculadas a la Agricultura (IFEVA-CONICET), Buenos Aires, Argentina.[80]Department of Environment and Society, Utah State University, Moab, UT, USA.[81]Universidad Nacional de Río Negro, Sede Atlántica, CEANPa, Río Negro, Argentina.[82]Cátedra de Manejo de Pastizales Naturales, Facultad de Ciencias Agrarias, Universidad Nacional de Catamarca, Catamarca, Argentina.[83]US Geological

Survey, Southwest Biological Science Center, Moab, UT, USA.[84]Instituto de Ecologia, INECOL, Chihuahua, Chihuahua, Mexico.[85]School of Sustainability, Arizona State University, Tempe, AZ, USA.[86]Al-Quds University, Palestine.[87]Department of Agriculture, Makhado, Limpopo, South Africa.[88]Sustainable Fibre Alliance, Grand Office, Ulaanbaatar, Mongolia.[89]The Dead-Sea and Arava Science Center, Yotvata, Israel.[90]Department of Geography and Earth Sciences. Aberystwyth University, Wales, UK.[91]School of Earth & Space Exploration, Arizona State University, Tempe, AZ, USA.[92]Science Division, Department of Planning, and Environment, New South Wales Government, Buronga, New South Wales, Australia.[93]ECOBIOSIS, Departement of Botany, University of Concepcion, Concepcion, Chile.[94]Zoology Department, National Museums of Kenya, Nairobi, Kenya.[95]Department of Earth and Environmental Sciences, Indiana University Indianapolis, Indianapolis, IN, USA.[96]Department of Natural Resources, Agricultural Research Organization, Institute of Plant Sciences, Gilat Research Center, Mobile Post Negev, Israel.[97]Kaye Academic College of Education, Beer Sheva, Israel.[98]State Key Laboratory of Desert and Oasis Ecology, Xinjiang Institute of Ecology and Geography, Chinese Academy of Sciences, Urumqi, China.

email: cesar.plaza@csic.es; eduardo.moreno@uam.es; fernando.maestregil@kaust.edu.sa

Mineral-associated organic carbon (MAOC) constitutes a major fraction of global soil carbon (C), and is assumed less sensitive to climate than particulate organic C (POC) due to protection by minerals. Despite its importance for long-term C storage, the response of MAOC to changing climates in drylands, which cover more than 40% of the global land area, remains unexplored. Here we assess topsoil organic C fractions across global drylands using a standardized field survey in 326 plots from 25 countries and six continents. We find that soil biogeochemistry explained the majority of variation in both MAOC and POC. Both C fractions decreased with increases in mean annual temperature and reductions in precipitation, with MAOC responding similarly to POC. Therefore, our results suggest that ongoing climate warming and aridification may result in unforeseen C losses across global drylands, and that the protective role of minerals may not dampen these effects.

Soils in drylands—the largest set of biomes of the planet —store 646 Pg of organic C, more than all living vegetation on Earth [1,2]. This vast soil organic C pool supports essential ecosystem services, including food provision and water and climate regulation for more than 2.5 billion people [3,4]. Yet, temperature increases and precipitation reductions forecasted for many dryland regions are expected to disrupt the balance of soil organic C, accelerating microbial decomposition, reducing plant C inputs into the soil, and resulting in more CO_2 emissions to the atmosphere [5,6].

The sensitivity of organic C in soils (sensu ref. [7]) to temperature and precipitation at timescales relevant to climate change mitigation is thought to be controlled largely by interactions with soil minerals, which restrict the accessibility of microbial decomposers by encapsulating and adsorbing organic matter [8–10]. Plant-derived materials at early stages of decomposition are the main constituents of the mineral-unprotected, particulate organic C (POC) fraction of soil organic matter [9]. The POC fraction is thus directly affected by changes in plant C inputs into the soil and is more exposed to microbial decomposition than the organic component of the mineral-associated organic C (MAOC) fraction, which has, therefore, a lower turnover rate [11,12]. As a result, large scale meta-analyses and observational studies suggest that POC is more sensitive to changes in climate, and particularly to warming, than MAOC [7,13–16]. Because of the typically large ratio of soil minerals to organic matter in drylands, MAOC is expected to dominate over POC, potentially driving a high persistence of soil organic C in these ecosystems [7,10,17]. However, no studies to date have examined the relationship of POC and MAOC with climate across the diverse environmental gradients that characterize global drylands. Investigating this relationship is particularly timely and relevant, as it would significantly reduce the uncertainty surrounding the land carbon-climate feedback. Additionally, it would provide valuable insights for adapting soil carbon-related ecosystem services to ongoing climate change.

Here we evaluated how mean annual temperature and precipitation relates to POC and MAOC contents across global drylands after accounting for major biotic (net primary productivity, vegetation type, woody cover, plant and herbivore richness, and grazing pressure) and soil biogeochemistry (clay and silt contents, pH, chemical index of alteration, exchangeable Ca, non-crystalline Al and Fe, available N and P, and microbial biomass C) factors known to potentially affect soil organic C content by regulating C inputs and stabilization processes [5,18]. To do so, we surveyed *in situ* 326 plots from 98 dryland ecosystems located in 25 countries from six continents (Extended Data Fig. 1). Our survey spans the broad gradients of temperature, precipitation, aridity, soil properties, vegetation types, and grazing pressures that can be found across drylands worldwide (Extended Data Tables 1 and 2) [19,20]. At each site, we collected topsoil samples (0-7.5 cm) from areas both covered (322) and not covered (326) by perennial vegetation from two to four plots located across a local gradient of extensive grazing pressure (648 samples in total, see Methods). We subjected all samples to a size fractionation procedure to separate and quantify C content in POC and MAOC pools [9,21]. Using these data, we tested the hypothesis that MAOC, being protected by minerals, is less sensitive than POC to increases in temperature and decreases in precipitation [7,10,16,22]. We also hypothesize that the presence of vegetation mitigates declines in soil C, particularly POC, by increasing soil C inputs.

MAOC dominates soil organic C and is sensitive to climate

Our results show that MAOC was the dominant soil organic C fraction in drylands globally (Fig. 1a). In particular, median MAOC content was 5.2 g C kg^{-1} soil, equivalent to 66% of the total soil organic C content, whereas median POC content was 2.3 g C kg^{-1} soil. This quantification falls within the range of soil organic C content (MAOC and POC) commonly found in drylands, and is relevant to improve the performance of emerging models of soil organic C formation and persistence using POC and MAOC frameworks [2, 23–25].

Contrary to our hypothesis, we found that MAOC and POC were equally sensitive to differences in climate across global drylands. In particular, both MAOC and POC were negatively associated with increasing temperature and decreasing precipitation to a similar extent, as indicated by the similar slopes of the associations (Fig. 1bc). These results were supported by the lack of a significant interaction between the effects of temperature and precipitation and the type of fraction (MAOC versus POC) tested by a linear mixed-effects model (Fig. 1d, see Methods). Based on the results from this model, we estimated that POC and

MAOC contents significantly declined with temperature at an average rate of 3.2% per ºC (95% confidence interval (CI): 1.8, 4.6) and increased with precipitation at an average rate of 6.6% per 100 mm (95% CI: 0.6, 12.6).

Warming accelerates the microbial decomposition of soil organic matter, and precipitation reduction constrains plant production and organic matter inputs into the soil [5,26]. Our results are, therefore, consistent with previously reported reductions in soil organic C content with increasing temperature and reducing precipitation across terrestrial ecosystems [27–29]. However, and contrary to expectations of smaller sensitivity of MAOC versus POC to changes in climate observed in more mesic systems [14,15], our findings based on a space-fir-time substitution highlight that the MAOC and POC fractions may decrease at similar rates in response to climate warming and precipitation reduction across global drylands. Therefore, they suggest that the current paradigm of mineral protection may not determine soil C persistence in dryland ecosystems [8,30–32]. The apparent lack of protection by minerals, which contrasts with what was observed in mesic systems richer in organic matter, was consistent across the range of soil organic C content found in drylands (Extended Data Fig. 2). There is recent evidence that MAOC is controlled not only by C stabilization in soil organo-mineral complexes, but also by changes in C inputs driven by climate [15]. In drylands, not only precipitation reduction but also warming may increase water deficit, which may decrease plant productivity [5], C inputs into the soil and C accumulation into the MAOC fraction. These is also evidence that dryland soils maintain a high oxidative potential during dry periods, mainly through the stabilization of enzymes, which result in a rapid organic matter decomposition in wet periods [28,29] and may further limit C inputs to the MAOC fraction.

Vegetation buffers soil C declines with warming

Both POC and MAOC contents were higher in soil beneath perennial vegetation (Fig. 2). We further observed that as mean annual temperature increased, POC and MAOC contents decreased, but to a lesser extent, beneath vegetation. Conversely, as mean annual precipitation increased, both contents increased in a similar manner in open areas and in areas under the canopy of perennial vegetation (Fig. 2). These results are important because they suggest that the presence of vegetation buffers, but does not fully compensate for, the negative effects of higher temperature on soil C fractions. While the buffering effect of vegetation did not completely counteract the vulnerability of organic C pools to increasing temperatures, our findings indicate that management practices aimed at protecting vegetation in drylands may help to maintain soil organic C stocks in global drylands and reducing their losses in response to a changing climate.

Coupling of POC and MAOC in drylands

We found that POC and MAOC contents were strongly correlated across global drylands ($r = 0.83$, $n = 326$, $P < 0.001$; Fig. 3a). These results strongly suggest that both fractions remain highly coupled in drylands despite their different levels of putative protection against decomposition by microorganisms.

Variance partitioning of linear mixed-effects models and random forest analysis showed that the order of importance of the group of factors that explained most of the variation of POC and MAOC across global drylands was essentially the same for both organic C fractions (Fig. 3b, Extended Data Fig. 3). Soil biogeochemistry, above climate and biotic factors, was the most important predictor of both POC and MAOC contents. Both C fractions were negatively associated with soil pH and positively associated to exchangeable Ca, available N and P, and microbial biomass C contents; additionally, MAOC was associated positively with clay and silt and non-crystalline Al and Fe contents (Extended Data Fig. 4). Slightly-acidic-to-neutral soils generally feature higher nutrient availability and more fertility than alkaline soils [33], which may thus favor soil organic C accumulation in drylands through increased plant-derived C inputs and microbial activity. The prevalent role of soil fine texture and non-crystalline Al and Fe in MAOC formation has been widely documented in the literature [31]. Sorption of organic matter to mineral surfaces is known to be promoted by the relatively high specific surface area and charge of clay and silt, while non-crystalline Fe and Al phases are also known to form strong associations with organic matter [31].

The coupling of POC and MAOC observed here for drylands may be, however, disrupted in more productive terrestrial ecosystems, where higher plant inputs may result in larger POC contents [13–15]. In contrast to experimental manipulation studies [14], our work addresses the vulnerability of soil C fractions using a space-for-time substitution. Further research into the pace of the climate-induced changes and the causality of the associations found in our study is thus warranted.

Concluding remarks

By using a global standardized field study and by focusing exclusively on dryland ecosystems, our work expands previous efforts to understand abiotic and biotic drivers of POC and MAOC along large geographical gradients, which have either been based on literature syntheses, which use datasets that are inherently heterogenous, or have focused on ecosystems other than drylands [16]. Our study generated highly standardized field data on the POC and MAOC fractions of dryland soils worldwide, along with their major predictors. These data significantly expand existing global databases and can be used to refine current soil organic C models.

Our findings suggest that ongoing changes in climate, particularly warming, may adversely affect both unprotected and mineral-protected soil C content in drylands to a similar extent. The results obtained also indicate that maintaining vegetation cover can mitigate, but not fully counteract, the negative impacts of rising temperatures on soil organic C fractions. Our study enhances our understanding of how POC and MAOC contents in soil respond to key abiotic and biotic drivers, revealing that mineral protection has limited potential to sustain organic C storage in dryland soils in the face of ongoing global warming. The novel insights about dryland soil C pools and their sensitivity provided here could facilitate much-needed advances in our model representation of dryland ecosystems and their response to climate change.

Acknowledgements

This research was funded by the European Research Council (ERC Grant agreement 647038, BIODESERT), the Spanish Ministry of Science and Innovation (PID2020-116578RB-I00), and Generalitat Valenciana (CIDEGENT/2018/041), with additional support by the University of Alicante (UADIF22-74 and VIGROB22-350). F.T.M. acknowledges support from the King Abdullah University of Science and Technology (KAUST) and the KAUST Climate and Livability Initiative. D.J.E. is supported by the Hermon Slade Foundation. L.W. acknowledges support from the US National Science Foundation (EAR 1554894). B.B. and S.S. were supported by the Taylor Family-Asia Foundation Endowed Chair in Ecology and Conservation Biology. MB acknowledges support from a Ramón y Cajal grant from the Spanish Ministry of Science

(RYC2021-031797-I). A.L. and L.K. acknowledge support from the German Research Foundation, DFG (grant CRC TRR228) and German Federal Government for Science and Education, BMBF (grants 01LL1802C and 01LC1821A). L.K. acknowledges travel funds from the Hans Merensky Foundation. A.N. and C.Br. acknowledge support from FCT - Fundação para a Ciência e a Tecnologia (CEECIND/02453/2018/CP1534/ CT0001, PTDC/ASP-SIL/7743/ 2020, UIDB/00329/2020), from AdaptForGrazing project (PRR-C05-i03-I-000035) and from LTsER Montado platform (LTER_EU_PT_001). S.C.R. was supported by NASA (NNH22OB92A) and is grateful to Erika Geiger, Armin Howell, Robin Reibold, Nick Melone, and Megan Starbuck for field support. Any use of trade, product, or firm names in this paper is for descriptive purposes only and does not imply endorsement by the U.S. Government. We thank the landowners for granting access to the sites and many people and their institutions for supporting our fieldwork activities: Louis Eloff, Dr Jorrie J. Jordaan, Dr Edwin Mudongo, Dr Vincent Mokoka, Baltimore Mokhou, Thabang Maphanga, Dr Dave Thompson (SAEON), Dr Anke S. K. Frank, Rose Matjea, Florian Hoffmann, Chris Goebel, the University of Limpopo, South African Environmental Observation Network (SAEON), the South African Military, and the Scientific Services Kruger National Park.

Author contributions

F.T.M. designed and coordinated the global field survey. C.P., F.T.M., and E.M.J. conceived this study. D.J.E., H.S., N.G., Y.L.B-P., B.G., V.O., E.G., M.G.G., E.V., S.A., M.B., J.M.V., B.J.M., W.F., N.E., S.C., M.A., R.J.A., J.M.A., F.A., V.A, A.I.A., K.B., F.B.S., N.B., B.B., M.A.B., D.B., C.Br., C.Bu., Y.C., R.Ca., A.P.C.M., I.C., P.C.Q., R.Ch., A.A.C., C.M.C., A.D.N., B.D., C.R.D., D.A.D., A.J.D., J.D., H.E., C.E., A.F., M.F., D.F., L.H., J.J.G., E.G.M., R.M.H.H., A.v.H., N.H., E.H.S., F.M.H., O.J.M., F.J., A.J., M.J., K.F.K., L.K., J.E.L., P.C.L.R., P.L., A.L., J.L., M.A.L., G.M.K., T.P.M., O.M.I., E.M., P.M., A.J.M., M.P.M., J.V.S.M., J.P.M., G.M., S.M.M., A.N., G.O., G.R.O., B.O., G.P., Y.P., R.E.Q., S.C.R., V.M.R., A.Ro., J.C.R., O.S., A.S., J.S., M.S., S.S., I.S., C.R.A.S., A.L.T., A.D.T., H.L.T., K.T., S.T., J.V., O.V., L.V.D.B., F.V., W.W., D.W., L.W., G.M.W., L.Y., E.Z., J.M.Z., Y.Z., and X.Z. performed field research. P.D.M., V.O., B.G., B.J.M., S.C., N.E., J.C.G.G., C.Z., M.P., W.F., I.B.F., A.Re., E.M.J., and C.P. conducted laboratory research and analysis. P.D.M., E.G., and C.P. carried out data analysis, after discussion, suggestions, and contributions from F.T.M., E.M.J., M.D.B., N.G., Y.L.B-P., H.S., C.Z., M.P., P.G.P., A.Re., M.B., and S.M.M. P.D.M. and C.P. wrote the original manuscript draft, with contributions from F.T.M., E.M.J., and M.D.B. All authors discussed the results and contributed to editing the manuscript.

Competing interests

The authors declare no competing interests.

Figure captions

Fig. 1 | Distribution of soil organic carbon (C) contents in particulate organic C (POC) and mineral-associated organic C (MAOC) fractions and their relationships with climate in global drylands. a, Boxplot of POC and MAOC contents. Box, 1st, and 3rd quartiles; central horizontal line, median; upper vertical line end, largest value smaller than 1.5 times the interquartile range; lower vertical line, smallest value larger than 1.5 times the interquartile range (n = 326 plots). **b-c**, Relationships between POC and MAOC contents and mean annual temperature (MAT, **b**) and precipitation (MAP, **c**). Lines and shading represent linear regressions and 95% confidence intervals. **d**, Summary of a linear mixed-effects model, controlling for biotic factors and soil biogeochemistry (see Methods). The panel shows coefficients (circles) and 95%

confidence intervals (CI, bars) for main and interaction effects of C fraction type (binary variable, either POC or MAOC) and climate (MAT and MAP) on POC and MAOC contents. The variance explained (R^2) by the fixed and random effects relative to the total variance was 77% and 12%, respectively (n = 634 POC and MAOC observations). Carbon fraction contents were natural-logarithm transformed, and all the predictors were standardized. The positive coefficient of C fraction type (MAOC vs. POC) indicate that MAOC contents are significantly greater than POC contents ($P < 0.001$). For the observed negative association of MAT and positive association of MAP with C content ($P < 0.001$ and $P = 0.039$ respectively), negative coefficients for the interaction of C fraction type with MAT and MAP indicate that increasing MAT has a stronger negative effect on MAOC than on POC contents ($P = 0.053$), while decreasing MAP has a stronger negative effect on POC than on MAOC ($P = 0.181$).

Fig. 2 | Relationships between climate and particulate organic C (POC) and mineral-associated organic C (MAOC) contents in soils under the canopy of the dominant perennial vegetation (V) and in open areas (O) across global drylands. a-d, Relationships between POC and mean annual temperature (MAT, **a**) and precipitation (MAP, **c**), and between MAOC and MAT (**b**) and MAP (**d**) in both O and V microsites. Lines and shading represent linear regressions and 95% confidence intervals (n = 326 and 322 for O and V, respectively). **e**, Coefficients (dots) and 95% confidence intervals (bars) of linear mixed-effects model illustrating the fixed main and interaction effects of MAT, MAP, and the presence of vegetation cover (V vs. O) on POC and MAOC contents (n = 648 V and O areas). The variance explained (R^2) by the fixed and random effects relative to the total variance was 30% and 55%, respectively, for POC, and 32% and 61%, respectively, for MAOC.

Fig. 3 | Coupling and drivers of particulate organic C (POC) and mineral-associated organic C (MAOC) in global drylands. a, Relationship between POC and MAOC contents. Dots represent individual dryland plots, with the colors of the dots illustrating their aridity (1 – annual precipitation/potential evapotranspiration) values. The line and shading represent the fitted linear regression and 95% confidence interval, respectively. **b**, Variance explained (R^2) by linear mixed-effects models for POC and MAOC contents partitioned into the fraction attributable to unique and shared among groups of drivers (climate: mean annual temperature and mean annual precipitation; biotic factors: net primary productivity, type of vegetation, woody cover, plant richness, grazing pressure, and herbivore richness; and soil biogeochemistry:

clay and silt, pH, chemical index of alteration, exchangeable Ca, non-crystalline Al and Fe, available N and P, and microbial biomass carbon). The variance explained (R^2) by the fixed and random effects relative to the total variance was 69% and 20% for POC (n = 317) and 84% and 11% for MAOC (n = 317), respectively.

References

1. IPCC. Global Carbon and Other Biogeochemical Cycles and Feedbacks. in Climate Change 2021 – The Physical Science Basis 673–816 (Cambridge University Press, 2023).
2. Plaza, C. et al. Soil resources and element stocks in drylands to face global issues. Sci Rep 8, (2018).
3. Maestre, F. T. et al. Structure and functioning of dryland ecosystems in a changing world. Annu Rev Ecol Evol Syst 47, 215–237 (2016).
4. Smith, P. et al. Biogeochemical cycles and biodiversity as key drivers of ecosystem services provided by soils. SOIL 1, 665–685 (2015).
5. Gaitán, J. J. et al. Biotic and abiotic drivers of topsoil organic carbon concentration in drylands have similar effects at regional and global scales. Ecosystems 22, 1445–1456 (2019).
6. Huang, J., Yu, H., Guan, X., Wang, G. & Guo, R. Accelerated dryland expansion under climate change. Nat Clim Chang 6, 166–171 (2016).
7. Lugato, E., Lavallee, J. M., Haddix, M. L., Panagos, P. & Cotrufo, M. F. Different climate sensitivity of particulate and mineral-associated soil organic matter. Nat Geosci 14, 295–300 (2021).
8. Hemingway, J. D. et al. Mineral protection regulates long-term global preservation of natural organic carbon. Nature 570, 228–231 (2019).
9. Lavallee, J. M., Soong, J. L. & Cotrufo, M. F. Conceptualizing soil organic matter into particulate and mineral-associated forms to address global change in the 21st century. Glob Chang Biol 26, 261–273 (2020).
10. Cotrufo, M. F. & Lavallee, J. M. Soil organic matter formation, persistence, and functioning: A synthesis of current understanding to inform its conservation and regeneration. in Advances in Agronomy (ed. Sparks, D. L.) vol. 172 1–66 (Academic Press, 2022).

11. Prairie, A. M., King, A. E. & Cotrufo, M. F. Restoring particulate and mineral-associated organic carbon through regenerative agriculture. Proceedings of the National Academy of Sciences 120, e2217481120 (2023).

12. Haddix, M. L., Paul, E. A. & Cotrufo, M. F. Dual, differential isotope labeling shows the preferential movement of labile plant constituents into mineral-bonded soil organic matter. Glob Chang Biol 22, 2301–2312 (2016).

13. Cotrufo, M. F., Ranalli, M. G., Haddix, M. L., Six, J. & Lugato, E. Soil carbon storage informed by particulate and mineral-associated organic matter. Nat Geosci 12, 989–994 (2019).

14. Rocci, K. S., Lavallee, J. M., Stewart, C. E. & Cotrufo, M. F. Soil organic carbon response to global environmental change depends on its distribution between mineral-associated and particulate organic matter: A meta-analysis. Sci Total Environ 793, 148569 (2021).

15. Hansen, P. M. et al. Distinct, direct and climate-mediated environmental controls on global particulate and mineral-associated organic carbon storage. Glob Chang Biol 30, e17080 (2024).

16. Georgiou, K. et al. Emergent temperature sensitivity of soil organic carbon driven by mineral associations. Nat Geosci 17, 205–212 (2024).

17. Cotrufo, F. M. et al. In-N-Out: A hierarchical framework to understand and predict soil carbon storage and nitrogen recycling. Glob Chang Biol 27, 4465–4468 (2021).

18. von Fromm, S. F. et al. Continental-scale controls on soil organic carbon across sub-Saharan Africa. SOIL 7, 305–332 (2021).

19. Maestre, F. T. et al. The BIODESERT survey: assessing the impacts of grazing on the structure and functioning of global drylands. Web Ecol 22, 75–96 (2022).

20. Maestre, F. T. et al. Grazing and ecosystem service delivery in global drylands. Science (1979) 378, 915–920 (2022).

21. Cambardella, C. A. & Elliot, E. T. Particulate soil organic-matter changes across a grassland cultivation sequence. Soil Science Society of America Journal 56, 777–783 (1992).

22. Cotrufo, M. F. et al. Formation of soil organic matter via biochemical and physical pathways of litter mass loss. Nat Geosci 8, 776–779 (2015).

23. Sokol, N. W. et al. Global distribution, formation and fate of mineral-associated soil organic matter under a changing climate: A trait-based perspective. Funct Ecol 36, 1411–1429 (2022).

24. Wieder, W. R. et al. Carbon cycle confidence and uncertainty: Exploring variation among soil biogeochemical models. Glob Chang Biol 24, 1563–1579 (2018).

25. Sulman, B. N. et al. Multiple models and experiments underscore large uncertainty in soil carbon dynamics. Biogeochemistry 141, 109–123 (2018).

26. Davidson, E. A. & Janssens, I. A. Temperature sensitivity of soil carbon decomposition and feedbacks to climate change. Nature 440, 165–173 (2006).

27. Smith, K. R. & Waring, B. G. Broad-scale patterns of soil carbon (C) pools and fluxes across semiarid ecosystems are linked to climate and soil texture. Ecosystems 22, 742–753 (2018).

28. Darrouzet-Nardi, A. et al. Consistent microbial and nutrient resource island patterns during monsoon rain in a Chihuahuan Desert bajada shrubland. Ecosphere 14, e4475 (2023).

29. Stursova, M. & Sinsabaugh, R. L. Stabilization of oxidative enzymes in desert soil may limit organic matter accumulation. Soil Biol Biochem 40, 550–553 (2008).

30. Lehmann, J. & Kleber, M. The contentious nature of soil organic matter. Nature 528, 60–68 (2015).

31. Kleber, M. et al. Mineral–Organic Associations: Formation, Properties, and Relevance in Soil Environments. in Advances in Agronomy (ed. Sparks, D. L.) vol. 130 1–140 (Academic Press, Waltham, MA, 2015).

32. Kleber, M. et al. Dynamic interactions at the mineral–organic matter interface. Nat Rev Earth Environ 2, 402–421 (2021).

33. Bardgett, R. D. The Biology of Soil: A Community and Ecosystem Approach. (Oxford University Press, United Kingdom, 2005).

Methods

Global field survey and soil sampling. Fieldwork was conducted from January 2016 to September 2019. A total of 326 plots distributed across 98 study sites in 25 countries from all continents except Antarctica (Algeria, Argentina, Australia, Botswana, Brazil, Canada, Chile, China, Ecuador, Hungary, Iran, Israel, Kazakhstan, Kenya, Mexico, Mongolia, Namibia, Niger, Palestine, Peru, Portugal, South Africa, Spain, Tunisia, and USA) and encompassing the wide range of vegetation, soil, climate, and grazing pressure levels found in drylands worldwide were surveyed using a common and standardized protocol [19,20].

At each site, we gathered field data within multiple 45 m x 45 m plots situated along a gradient of grazing pressure, encompassing high (n = 98), medium (n = 97), and low (n = 88) pressure levels, as well as ungrazed areas (n = 43). To establish the grazing gradients, in 90 out of the 98 sites surveyed, we strategically positioned these plots at varying distances from artificial watering points, which are usually created in drylands to supply introduced livestock with permanent water sources [34]. The closer the plot to the permanent water source, the more intense the grazing [34,35]. In the remaining eight sites, local variations in grazing pressure gradients were ascertained by observing different paddocks featuring varying grazing intensities. See ref. [20] for additional details on the characterization and validation of the local grazing pressure gradients established.

A portable Global Positioning System was used to record the coordinates and elevation of each plot, which were standardized to the WGS84 ellipsoid for visualization and analyses. During the dry season at each site, four soil cores (145 cm^3) from 0 to 7.5-cm depth (topsoil) were collected from five 50 × 50-cm quadrats randomly placed in areas under the canopy of the dominant perennial vegetation and five placed in open areas not covered by perennial vegetation.

The soil cores were homogenized and composited to form a sample representative of the soil under the dominant vegetation and a sample representative of the soil in open areas within each plot. The soil samples were passed through a 2-mm sieve. A portion of each soil sample was air-dried and used for organic matter fractionation and texture and pH analysis, and another portion was stored at -20 °C and used for microbial biomass C analysis. A portion of the air-dried soil samples was ground with a ball mill for additional chemical analysis.

Soil organic carbon fractionation and quantification. All the soil samples, a total of 648 (326 from open areas and 322 from under the canopy of the dominant vegetation), were subjected to a size fractionation method [21,36] to separate the POC (not protected by minerals from microbial decomposition) and MAOC (protected by minerals) fractions. Aggregates were dispersed by adding 30 mL of sodium hexametaphosphate (5 g L^{-1}) to 10 g of soil and shaking with an overhead shaker for 18 h. After dispersion, the mixture was thoroughly rinsed through a 53-µm sieve, to separate the POC (> 53 µm) and MAOC (< 53 µm) fractions using an automated wet sieving system. The isolated fractions were oven-dried at 60 ºC, weighed, and ground with a ball mill. The whole soil samples and the POC and MAOC fractions were analyzed for organic C contents by dry combustion and gas chromatography using a ThermoFlash 2000 NC Soil Analyzer (Thermo Fisher Scientific, MA) after removing carbonates by acid fumigation [37].

Climate data. Mean annual temperature and mean annual precipitation data were obtained from WorldClim 2.0 [38] a high resolution (30 arc seconds or ~ 1 km at the equator) database based on a large number of climate observations and topographical data for the 1970-2000 period. Aridity index (ratio of average annual precipitation to potential evapotranspiration) data were obtained from the Global Aridity Index and Potential Evapotranspiration Climate Database v3 [39]. Aridity was calculated as 1 – aridity index.

Vegetation and herbivore richness survey. Each plot was classified as grassland, shrubland, or forest by identifying the dominant type of vegetation. Net primary productivity (NPP) was estimated using the mean annual Normalized Difference Vegetation Index (NDVI) averaged monthly values between 1999 and 2019 at a resolution of 30 m from Landsat 7 Enhanced Thematic Mapper Plus (ETM+) [40]. The cover of perennial vascular plants (plant cover) was measured along four parallel 45-m transects separated by 10 m and oriented downslope during the peak of the growing season using the line-intercept method [19,41,42]. Woody cover was measured in 25 contiguous quadrats (1.5 m × 1.5 m) placed in each transect (100 quadrats per plot). Plant richness was the total number of unique perennial species found along the quadrats and transects surveyed. The richness of herbivores was quantified at each plot using dung data collected systematically in situ along the four 45-m transects established as described in ref. [20].

Soil analyses. All the bulk soil samples were analyzed as follows. Clay and silt contents were determined by sieving and sedimentation [43]. Soil pH was measured in a water suspension at a soil-to-water ratio of 1:2.5 [44]. The chemical index of alteration, which is an indicator of the degree of weathering, was calculated as the molecular proportion of Al_2O_3 versus $Al_2O_3 + CaO + Na_2O + K_2O$ [45], using total Al, Ca, Na, and K contents and after correcting Ca for soils with carbonates [18]; total Al, Ca, Na and K contents were determined by inductively coupled plasma atomic emission spectroscopy (ICP-AES) after digestion in nitric and perchloric acids [44,46]. Exchangeable Ca content was determined by ICP-AES after extraction with ammonium acetate at pH 7.0 [44,47]. Non-crystalline Fe and Al contents were determined by ICP-AES after extraction with acid ammonium oxalate [48]. Available N (ammonium and nitrate) content was determined by extraction with 0.5 M K_2SO_4 and the indophenol blue method using a microplate reader [49].

Available P content was determined by the Olsen method [50]. Microbial biomass C was determined by substrate-induced respiration [51] using an automated microrespirometer [52].

Statistical analyses. We compared the content of MAOC with that of POC in global dryland soils controlling for confounding factors, and tested the hypothesis that the effects of climate (mean annual temperature and precipitation) on POC and MAOC contents depends on (interacts with) the C fraction type. For these analyses, we aggregated soil data for open and vegetation covered areas by plot using plant cover area as a weighting factor, and fitted a linear mixed-effects model on the response of C content with C fraction type as a binary categorical predictor (either MAOC or POC). In the fixed-effects term of the model, we also included mean annual temperature, mean annual precipitation, and the interactions of mean annual temperature and mean annual precipitation with C fraction type, as well as key biotic (net primary productivity, type of vegetation, woody cover, plant richness, grazing pressure, and herbivore richness) and soil biogeochemical (clay and silt, pH, chemical index of alteration, exchangeable Ca, non-crystalline Al and Fe, available N and P, and microbial biomass C) covariates to control for confounding factors. In the random term of the model, we incorporated an intercept structure with plot nested within site as a categorical variable to account for the lack of independence in the residuals due to the paired POC and MAOC separation and the plot sampling design. We checked whether the fit of this linear mixed-effects model improved by including quadratic terms of mean annual temperature, mean annual precipitation, and both mean annual temperature and precipitation, using the Akaike information criterion (AIC) and likelihood ratio tests. None of the quadratic models tested was a significantly better fit to the data (χ^2 (1) < 1.0, P > 0.3) than the linear model (lowest AIC).

To examine separately the variance of POC and MAOC contents explained by the groups of predictors (climate: mean annual temperature and mean annual precipitation; biotic factors: net primary productivity, type of vegetation, woody cover, plant richness, grazing pressure, and herbivore richness; soil biogeochemistry: clay and silt, pH, chemical index of alteration, exchangeable Ca, non-crystalline Al and Fe, available N and P, and microbial biomass C), we built two linear mixed-effects models (one for POC and another one for MAOC) with site as a random categorical variable. These two separate models were used to assess the importance of the different groups of predictors in explaining either POC or MAOC, and not to test statistically for differences in the size of the effects of the predictors between POC and MAOC. To support the linear mixed-effects models, we tested the importance of the same groups of predictors of POC and MAOC using random forest regression modeling [53]. In particular, we built two random forest models, one for POC and one for MAOC, combining 500 trees, and quantified the importance of each predictor by computing the increase in mean squared error across trees when the predictor was permuted.

We tested whether the presence of vegetation cover interacted with the effects of temperature and precipitation also by linear mixed-effects modeling. For this purpose, we built two linear mixed-effects models, one for POC content and another one for MAOC content in areas under the canopy of the dominant perennial vegetation and open areas, with vegetation cover as a binary predictor and plot nested within site in the random term.

For all the linear mixed-effects models, POC, MAOC, exchangeable Ca, non-crystalline Al and Fe, available N and P, and microbial biomass C were natural-logarithm transformed to reduce the skewness of the data. To compare effect sizes, all the numeric predictors were standardized by subtracting the mean and dividing by two standard deviations, and the binary variables (C fraction type and vegetated vs. open areas) were rescaled to -0.5 and 0.5 [54]. The coefficients of the models were estimated by the restricted maximum likelihood approach, 95% confidence intervals were calculated, and P-values were computed based on Satterthwaite approximation [55]. The validity of the assumptions of normality, homoscedasticity and linearity were examined using residual plots. The generalized variance inflation factors (GVIFs) were computed to check for multicollinearity among predictors (GVIF values were less than 3 in all cases, suggesting that multicollinearity was low [56]). All statistical analyses were performed using R [57] and the R packages arm [58], ggplot2 [59], lme4 [60], lmerTest [55], partR2 [61], patchwork [62], rnaturalearth [63], randomForest [64], sf [65], terra [66], and viridis [67].

Data availability

The data associated with this study are publicly available in https://figshare.com/s/8aeac2300650181f2c86 (https://doi.org/10.6084/m9.figshare.24678891) [68].

Methods-only references

34. Fensham, R. J. & Fairfax, R. J. Water-remoteness for grazing relief in Australian arid-lands. Biol Conserv 141, 1447–1460 (2008).
35. Fensham, R. J., Fairfax, R. J. & Dwyer, J. M. Vegetation responses to the first 20 years of cattle grazing in an Australian desert. Ecology 91, 681–692 (2010).
36. Sokol, N. W. & Bradford, M. A. Microbial formation of stable soil carbon is more efficient from belowground than aboveground input. Nat Geosci 12, 46–53 (2019).
37. Harris, D., Horwáth, W. R. & Van Kessel, C. Acid fumigation of soils to remove carbonates prior to total organic carbon or carbon-13 isotopic analysis. Soil Sci Soc Am J 65, 1853–1856 (2001).
38. Fick, S. E. & Hijmans, R. J. WorldClim 2: new 1-km spatial resolution climate surfaces for global land areas. Int J Climatol 37, 4302–4315 (2017).

39. Zomer, R. J., Xu, J. & Trabucco, A. Version 3 of the Global Aridity Index and Potential Evapotranspiration Database. Sci Data 9, 409 (2022).
40. Vermote, E., Justice, C., Claverie, M. & Franch, B. Preliminary analysis of the performance of the Landsat 8/OLI land surface reflectance product. Remote Sens Environ 185, 46–56 (2016).
41. Levi, E. B. & Madden, E. A. The point method of pasture analysis. New Zealand J. Agric. 46, 267–279 (1933).
42. Maestre, F. T. et al. Plant species richness and ecosystem multifunctionality in global drylands. Science (1979) 335, 214–218 (2012).
43. Kettler, T. A., Doran, J. W. & Gilbert, T. L. Simplified method for soil particle-size determination to accompany soil-quality analyses. Soil Sci Soc Am J 65, 849–852 (2001).
44. Sparks, D. L. et al. Methods of Soil Analyses, Part 3: Chemical Methods. (Soil Science Society of America, American Society of Agronomy, 1996).
45. Nesbitt, H. W. & Young, G. M. Early proterozoic climates and plate motions inferred from major element chemistry of lutites. Nature 299, 715–717 (1982).
46. Hesse, P. R. A Textbook of Soil Chemical Analysis. (John Murray, London, 1971).
47. Rasmussen, C. et al. Beyond clay: towards an improved set of variables for predicting soil organic matter content. Biogeochemistry 137, 297–306 (2018).
48. Darke, A. K. & Walbridge, M. R. Estimating non-crystalline and crystalline aluminum and iron by selective dissolution in a riparian forest soil. Commun Soil Sci Plant Anal 25, 2089–2101 (1994).
49. Sims, G. K., Ellsworth, T. R. & Mulvaney, R. L. Microscale determination of inorganic nitrogen in water and soil extracts. Commun Soil Sci Plant Anal 26, 303–316 (1995).
50. Olsen, S. R. & Sommers, L. E. Phosphorus. in Methods of Soil Analysis. Part 2. Chemical and Microbiological Properties (eds. Page, A. L., Miller, R. H. & Keeney, D. R.) 403–430 (American Society of Agronomy and Soil Science Society of America, Madison, WI, 1982).
51. Anderson, J. P. E. & Domsch, K. H. A physiological method for the quantitative measurement of microbial biomass in soils. Soil Biol Biochem 10, 215–221 (1978).
52. Scheu, S. Automated measurement of the respiratory response of soil microcompartments: Active microbial biomass in earthworm faeces. Soil Biol Biochem 24, 1113–1118 (1992).
53. Breiman, L. Random forests. Mach Learn 45, 5–32 (2001).

54. Gelman, A. Scaling regression inputs by dividing by two standard deviations. Stat Med 27, 2865–2873 (2008).

55. Kuznetsova, A., Brockhoff, P. B. & Christensen, R. H. B. lmerTest package: Tests in linear mixed effects models. J Stat Softw 82, 1–26 (2017).

56. James, G., Witten, D., Hastie, T. & Tibshirani, R. An Introduction to Statistical Learning. vol. 112 (Springer, 2013).

57. R Core Team. R: A Language and Environment for Statistical Computing. Preprint at https://www.R-project.org/ (2023).

58. Gelman, A. & Su, Y.-S. arm: Data Analysis Using Regression and Multilevel/Hierarchical Models. Preprint at https://CRAN.R-project.org/package=arm (2022).

59. Wickham, H. Ggplot2: Elegant Graphics for Data Analysis. (Springer-Verlag New York, 2016).

60. Bates, D., Mächler, M., Bolker, B. M. & Walker, S. C. Fitting linear mixed-effects models using lme4. J Stat Softw 67, 1–48 (2015).

61. Stoffel, M. A., Nakagawa, S. & Schielzeth, H. partR2: Partitioning R2 in generalized linear mixed models. bioRxiv (2020) doi:10.1101/2020.07.26.221168.

62. Pedersen, T. L. patchwork: The Composer of Plots. R package version 1.1.1. https://CRAN.R-project.org/package=patchwork. Preprint at https://cran.r-project.org/package=patchwork (2020).

63. Massicotte, P. & South, A. rnaturalearth: World Map Data from Natural Earth. Preprint at https://CRAN.R-project.org/package=rnaturalearth (2023).

64. Liaw, A. & Wiener, M. Classification and Regression by randomForest. R News 2, 18–22 (2002).

65. Pebesma, E. & Bivand, R. Spatial Data Science: With Applications in R. (Chapman and Hall/CRC, 2023).

66. Hijmans, R. J. terra: Spatial Data Analysis. Preprint at https://CRAN.R-project.org/package=terra (2023).

67. Garnier, S. viridis: Default Color Maps from ‘matplotlib’. Preprint at https://cran.r-project.org/package=viridis (2018).

68. Díaz-Martínez, P, Maestre, F.T., Moreno-Jiménez, E. & Plaza, C. Data from Vulnerability of mineral-associated soil organic carbon to climate in global drylands. Figshare. https://doi.org/10.6084/m9.figshare.24678891 (2024).

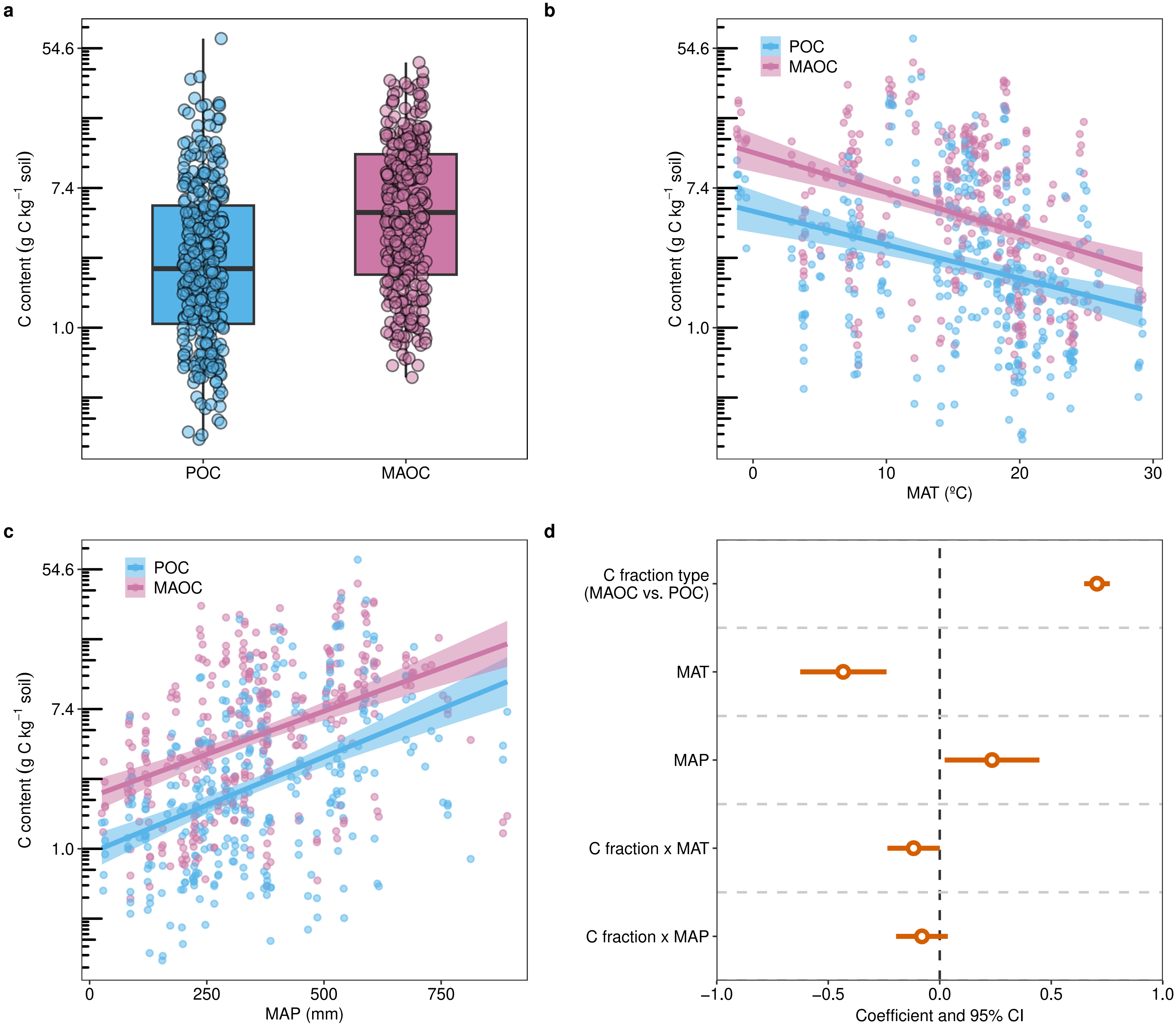
a
54.6
7.4
1.0
C content (g C kg^{-1} soil)
POC
MAOC
b
POC
MAOC
54.6
7.4
1.0
C content (g C kg^{-1} soil)
0
10
20
30
MAT (ºC)
c
POC
MAOC
54.6
7.4
1.0
C content (g C kg^{-1} soil)
0
250
500
750
MAP (mm)
d
C fraction type (MAOC vs. POC)
MAT
MAP
C fraction x MAT
C fraction x MAP
−1.0
−0.5
0.0
0.5
1.0
Coefficient and 95% CI

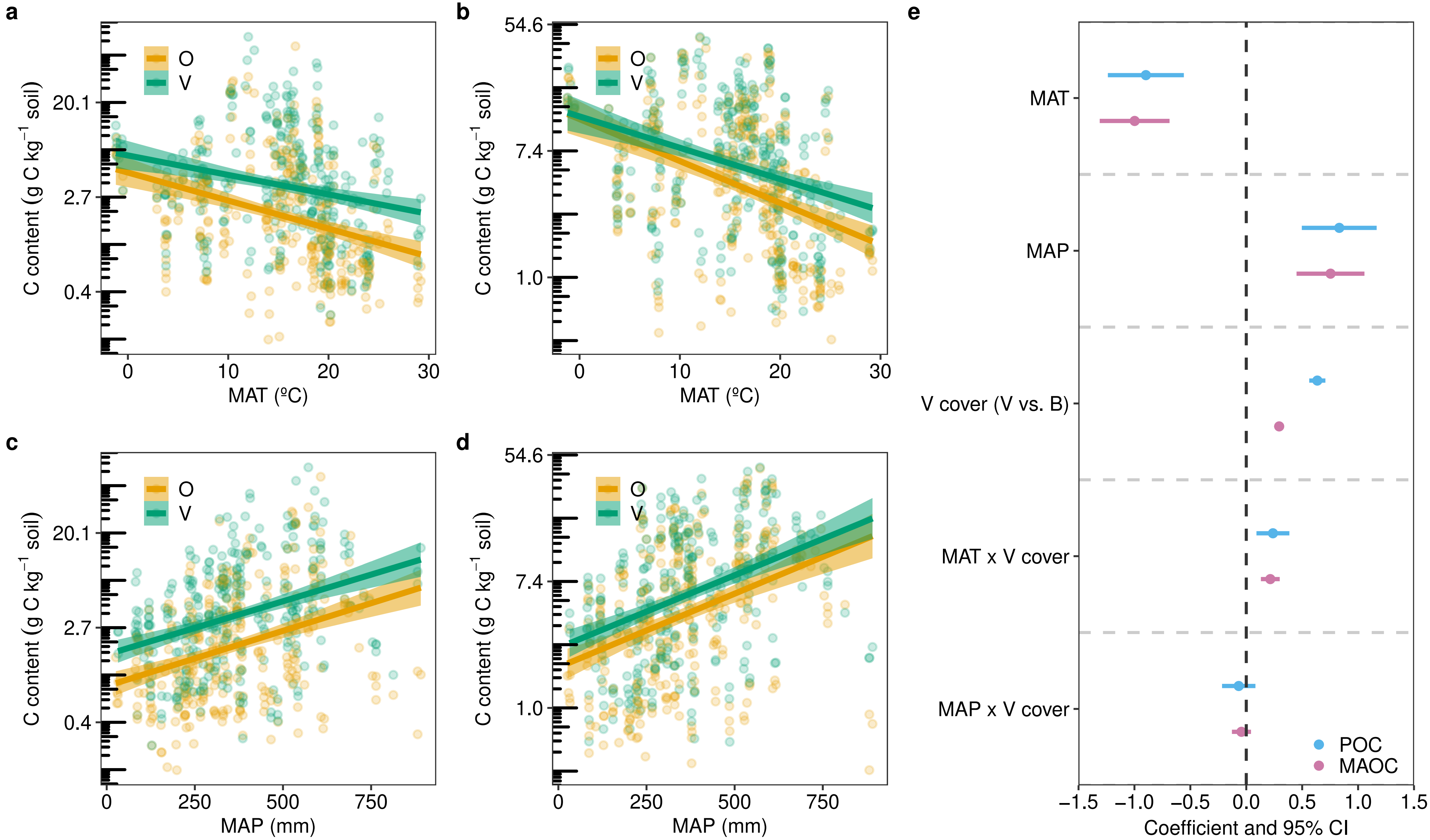
a
b
c
d
e
O
V
C content (g C kg^{-1} soil)
20.1
2.7
0.4
54.6
7.4
1.0
MAT (ºC)
0
10
20
30
MAP (mm)
250
500
750
MAT
MAP
V cover (V vs. B)
MAT x V cover
MAP x V cover
POC
MAOC
−1.5
−1.0
−0.5
0.0
0.5
1.0
1.5
Coefficient and 95% CI

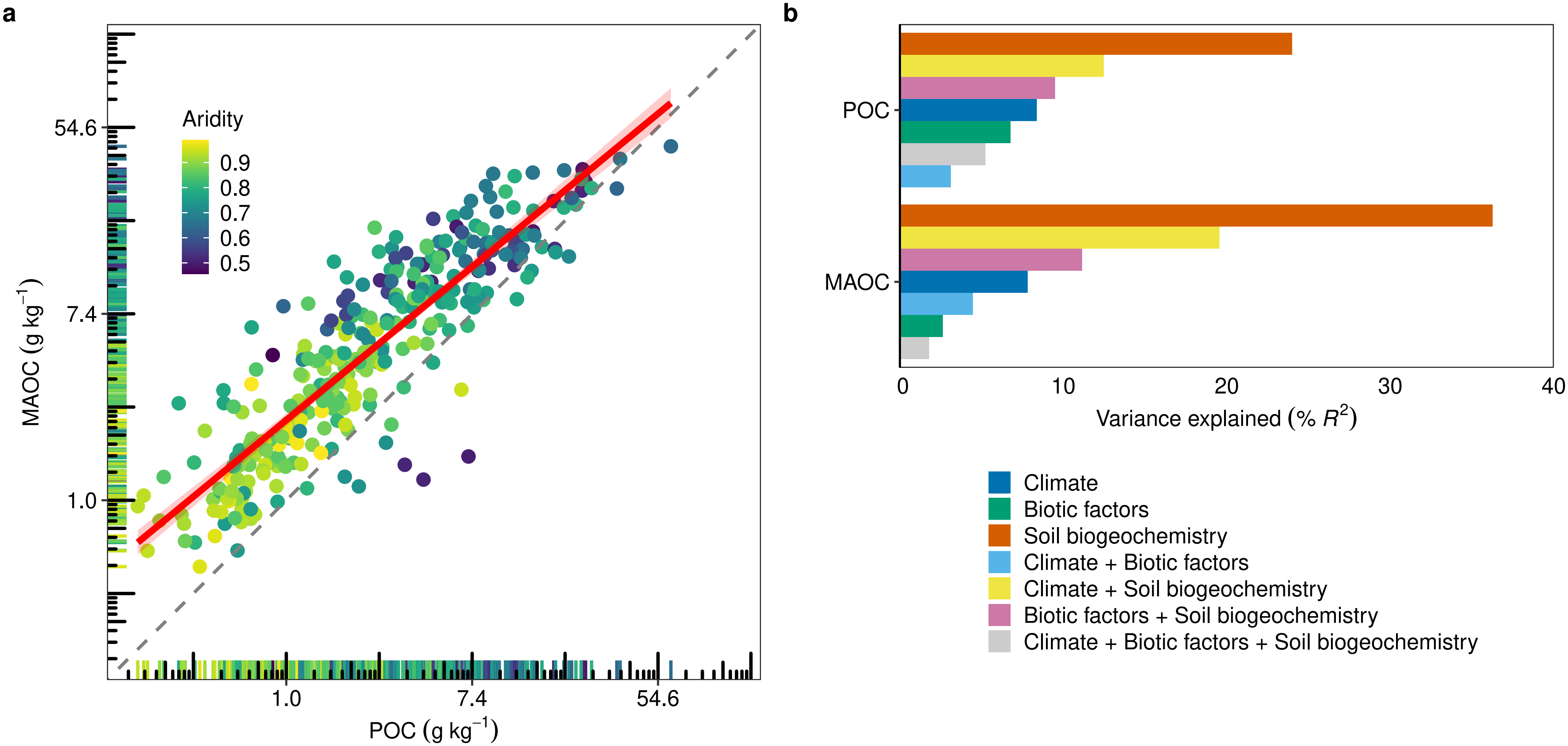
a
Aridity
0.9
0.8
0.7
0.6
0.5
MAOC (g kg^{-1})
54.6
7.4
1.0
1.0
7.4
54.6
POC (g kg^{-1})
b
POC
MAOC
0
10
20
30
40
Variance explained (% R^2)
Climate
Biotic factors
Soil biogeochemistry
Climate + Biotic factors
Climate + Soil biogeochemistry
Biotic factors + Soil biogeochemistry
Climate + Biotic factors + Soil biogeochemistry

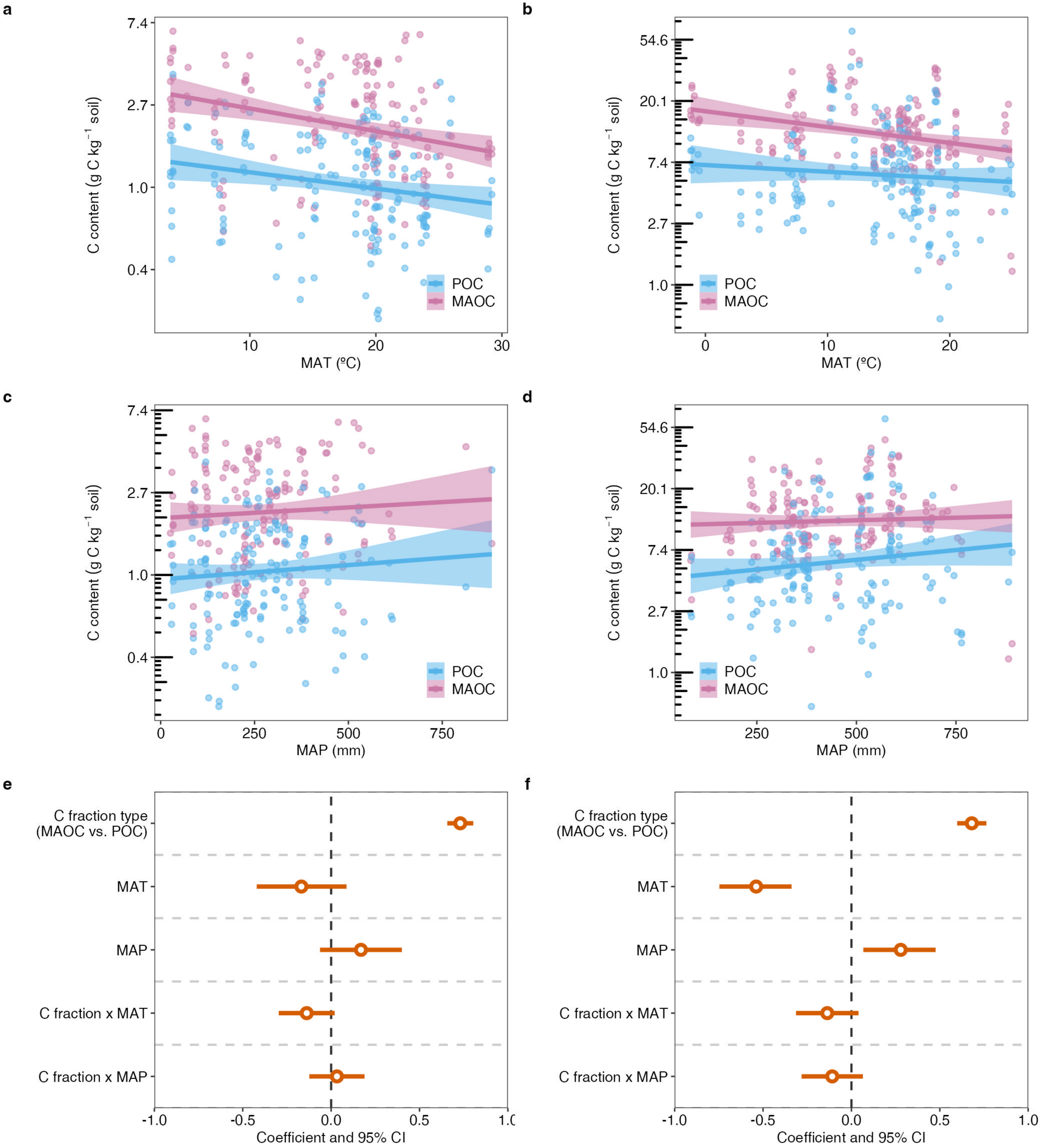
a
b
c
d
e
f
C content (g C kg^{-1} soil)
7.4
2.7
1.0
0.4
54.6
20.1
MAT (ºC)
MAP (mm)
0
10
20
30
250
500
750
POC
MAOC
C fraction type (MAOC vs. POC)
MAT
MAP
C fraction x MAT
C fraction x MAP
Coefficient and 95% CI
-1.0
-0.5
0.0
0.5
1.0

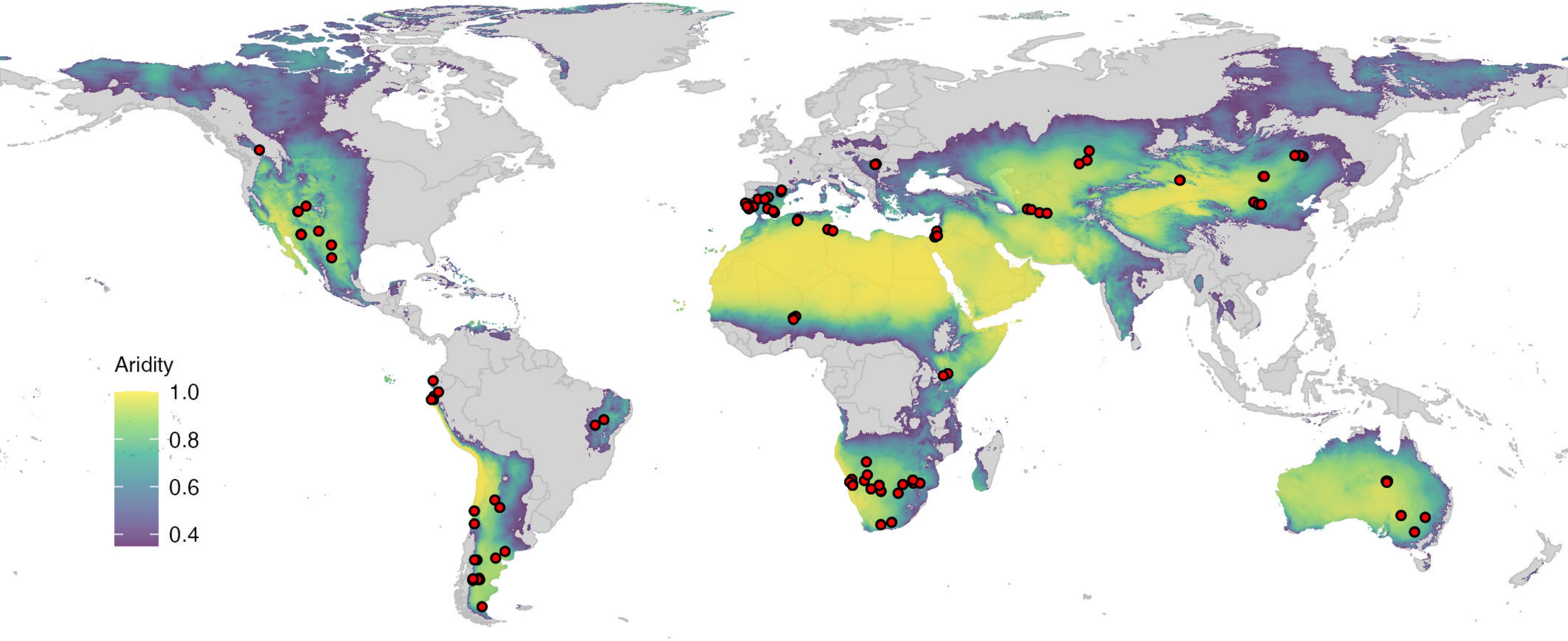
Aridity
1.0
0.8
0.6
0.4

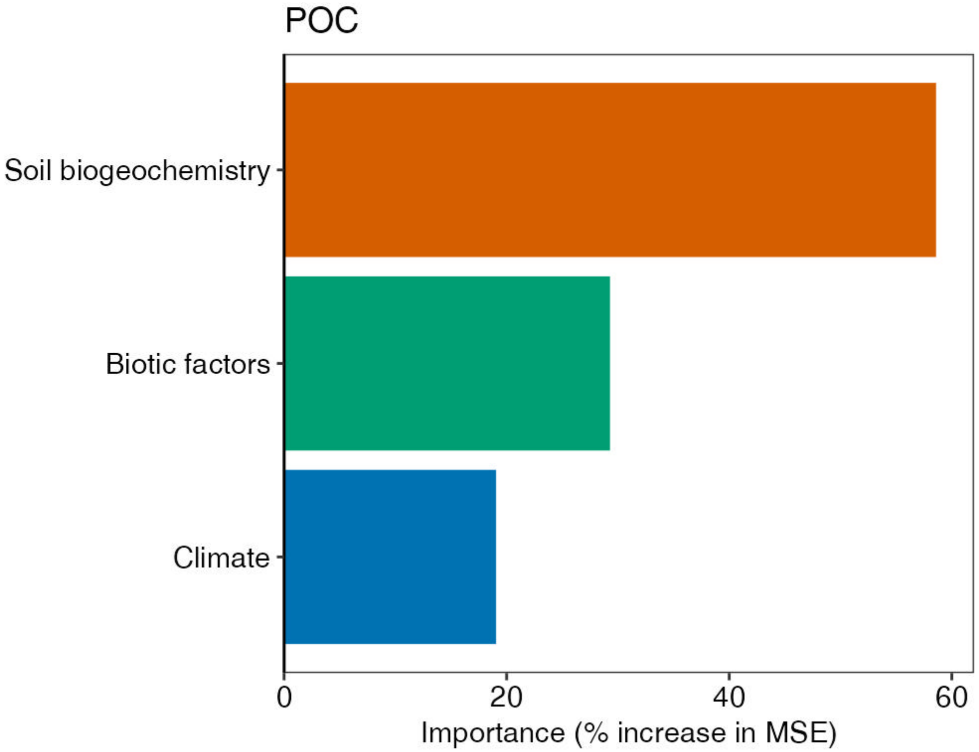
POC
Soil biogeochemistry
Biotic factors
Climate
0
20
40
60
Importance (% increase in MSE)

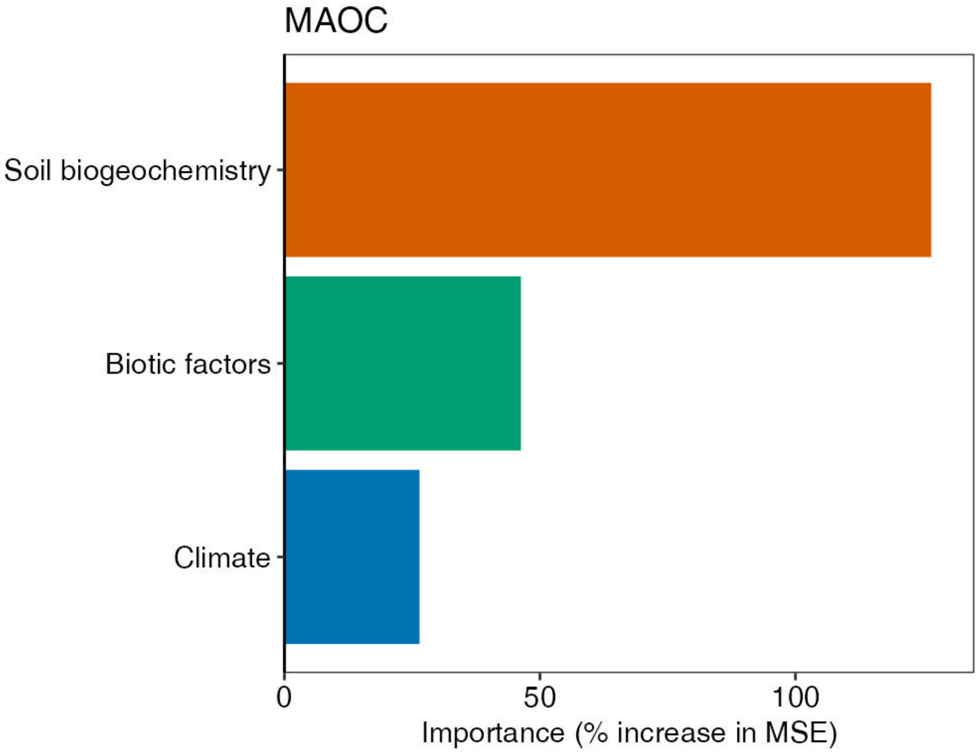
MAOC
Soil biogeochemistry
Biotic factors
Climate
0
50
100
Importance (% increase in MSE)

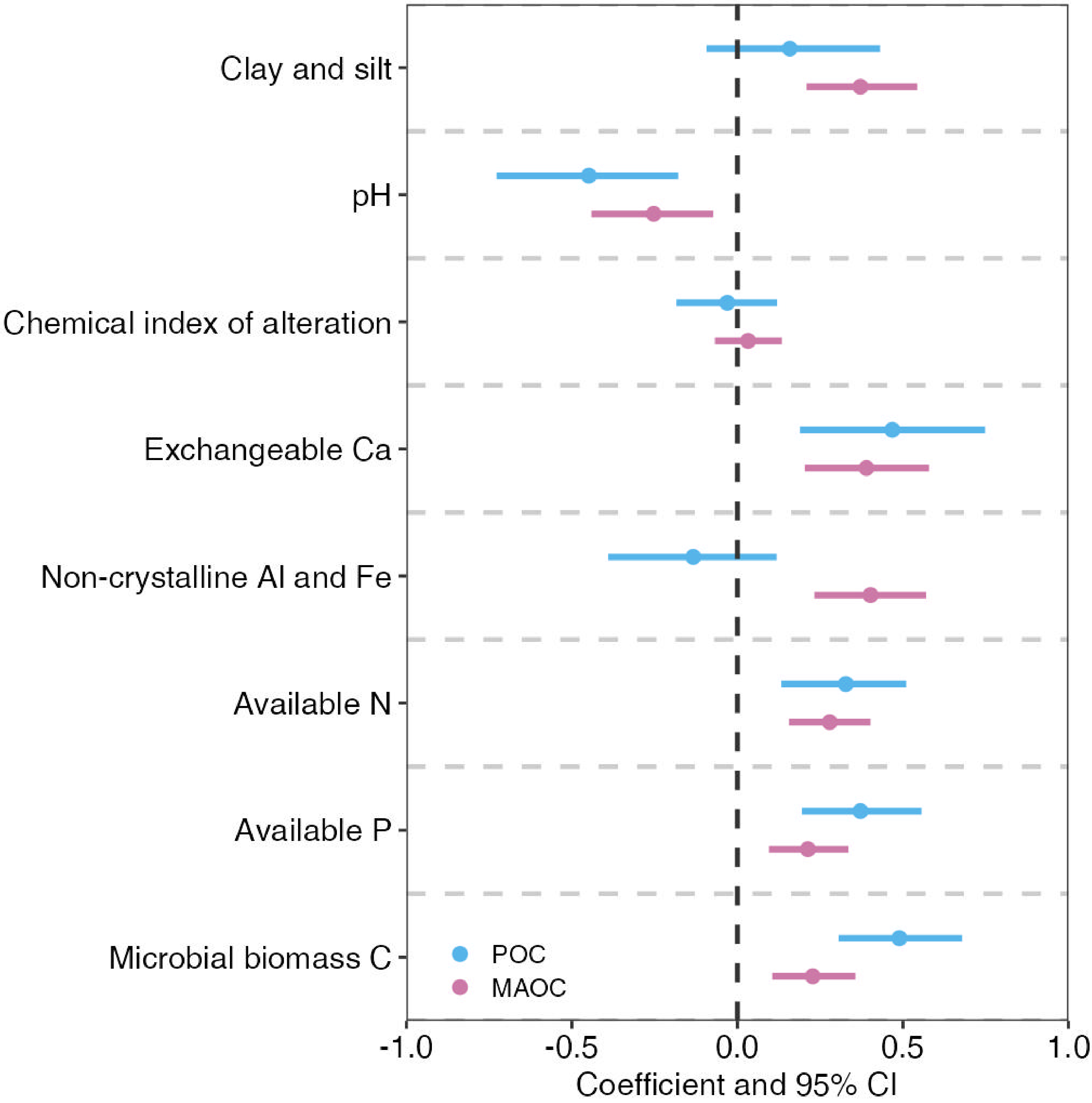
Clay and silt
pH
Chemical index of alteration
Exchangeable Ca
Non-crystalline Al and Fe
Available N
Available P
Microbial biomass C
● POC
● MAOC
-1.0
-0.5
0.0
0.5
1.0
Coefficient and 95% CI

Variable	**n**	**Min**	**Q1**	**Median**	**Mean**	**Q3**	**Max**
MAT (ºC)	326	-1.2	10.4	16.6	15.5	19.9	29.2
MAP (mm)	326	26	233	332	357	505	891
Net primary productivity (NDVI, unitless)	326	0.06	0.13	0.17	0.19	0.25	0.43
Woody cover (%)	326	0	15	46	48	83	100
Plant richness (number of species)	326	0	8	16	19	26	57
Herbivore richness (number of species)	326	0	1	2	2	3	6
Clay and silt (g kg^{-1})	326	10	120	271	325	512	870
pH	326	4.5	6.1	7.0	6.9	7.8	9.9
Chemical index of alteration (%)	326	42	74	81	79	87	97
Exchangeable Ca (mg kg^{-1})	321	39	843	1730	3394	3443	42446
Non-crystalline Al and Fe (mg kg^{-1})	326	28	475	932	1357	1620	9889
Available N (mg kg^{-1})	326	1	8	14	21	26	143
Available P (mg kg^{-1})	323	0.1	5.5	11.5	13.6	17.8	87.6
Microbial biomass C (mg kg^{-1})	326	16	101	186	245	331	1065

Variable	**Category**	**Number of observations**
Vegetation type	Grassland	94
	Shrubland	160
	Forest	72
Grazing pressure	Zero	43
	Low	88
	Medium	97
	High	98